

# Homologous states in $^{139,140}\text{Pr}$ via the $^{142,143}\text{Nd}(\vec{p}, \alpha)^{139,140}\text{Pr}$ reactions

**P Guazzoni<sup>1</sup>, L Zetta<sup>1</sup>, T Faestermann<sup>2</sup>, R Hertenberger<sup>3</sup>, H F Wirth<sup>3</sup>  
and M Jaskola<sup>4</sup>**

<sup>1</sup> Dipartimento di Fisica dell'Università degli Studi and I.N.F.N. I–20133 Milano, Italy

<sup>2</sup> Physik Department TUM, D–85748 Garching, Germany

<sup>3</sup> Fakultät für Physik der LMU, D–85748 Garching, Germany

<sup>4</sup> Soltan Institute for Nuclear Studies, 00–681 Warsaw, Poland

E-mail: paolo.guazzoni@mi.infn.it

**Abstract.** In order to study the spectator role of the  $f_{7/2}$  unpaired neutron outside the  $N=82$  closed shell in  $^{143}\text{Nd}$ , the  $^{142,143}\text{Nd}(\vec{p}, \alpha)^{139,140}\text{Pr}$  reactions have been measured in high resolution experiments at 23.5 MeV incident proton energy from the Munich MP Tandem accelerator, using the Stern–Gerlach type polarized hydrogen ion source and the Q3D magnetic spectrograph. Multiplets of states of  $^{140}\text{Pr}$ , homologous to the low-lying states of  $^{139}\text{Pr}$  have been identified in  $J^\pi$ .

## 1. Introduction

The  $(p, \alpha)$  reactions induced on target nuclei having one unpaired nucleon outside a magic shell are characterized by some distinctive features, which can be explained by assuming a weakly coupling to the magic core of this last, slightly bound nucleon, that acts as a spectator in the process.

These features are:

a) the weak population of residual nucleus levels below an excitation energy strictly related to the energy gap in the nucleon state spacing at the filling of the magic shell;

b) the excitation of homologous states (states with a close structural relationship) of residual nuclei from  $(p, \alpha)$  reactions on neighbouring systems, one magic with a magic neutron and /or proton shell and the other near magic with one more nucleon outside the magic shell.

This behaviour implies the persistence of preferred structures that survive after the addition of a spectator particle, so that the reaction takes place mainly with the core. This explains the great similarity between the spectra for each pair of reactions; they have almost the same shape but are shifted by an energy amount that corresponds to the gap between unpaired nucleon and closed shell, as we have shown in previous studies of the  $(p, \alpha)$  reaction, based on a low resolution experiment [1]. We have already tested this behaviour in the  $Z=20, 40, 50$  and  $82$  regions [2–6].

In order to investigate the spectator role of the  $f_{7/2}$  unpaired neutron outside the  $N=82$  closed shell in  $^{143}\text{Nd}$  and to test once again the validity of the homology concept also in this region, the  $^{142,143}\text{Nd}(\vec{p}, \alpha)^{139,140}\text{Pr}$  reactions have been studied. For the  $^{142,143}\text{Nd}(\vec{p}, \alpha)^{139,140}\text{Pr}$  reactions, the gap between the  $f_{7/2}$  neutron level above the  $N=82$  magic shell and  $d_{3/2}$  level which completes this shell can be estimated from the excitation energy of the first  $7/2^-$  excited state of  $^{137}\text{Ba}$  which is strongly

populated in the  $^{136}\text{Ba}(d,p)^{137}\text{Ba}$  reaction and amounts to 1.79 MeV [7] in good agreement with our experimental finding.

## 2. The experiment and the results

The  $^{142,143}\text{Nd}(p,\alpha)^{139,140}\text{Pr}$  reactions have been measured at 23.5 MeV incident proton energy from the Munich MP Tandem accelerator and the Stern–Gerlach atomic beam source of negative polarized hydrogen source [8]. The proton beam current intensity was up to 1.5  $\mu\text{A}$  and the beam polarization  $\sim 60\%$ . Isotopically enriched targets of  $^{142,143}\text{Nd}_2\text{O}_3$  (98.26% and 91.68% respectively)  $82 \mu\text{g}/\text{cm}^2$  thick were evaporated on a  $8 \mu\text{g}/\text{cm}^2$  carbon backing. The reaction products were analyzed with the Q3D magnetic spectrograph and detected by the focal plane detector with cathode readout [9]. To provide the energy calibration of the  $^{139,140}\text{Pr}$  spectra, the  $^{123}\text{Sb}(p,\alpha)^{120}\text{Sn}$  reaction [5] has been used. The angular distributions of cross sections  $\sigma(\theta)$  and analyzing powers  $A_y(\theta)$  of the triton pickup reactions  $^{142,143}\text{Nd}(p,\alpha)^{139,140}\text{Pr}$  have been measured from  $10^\circ$  to  $60^\circ$ .

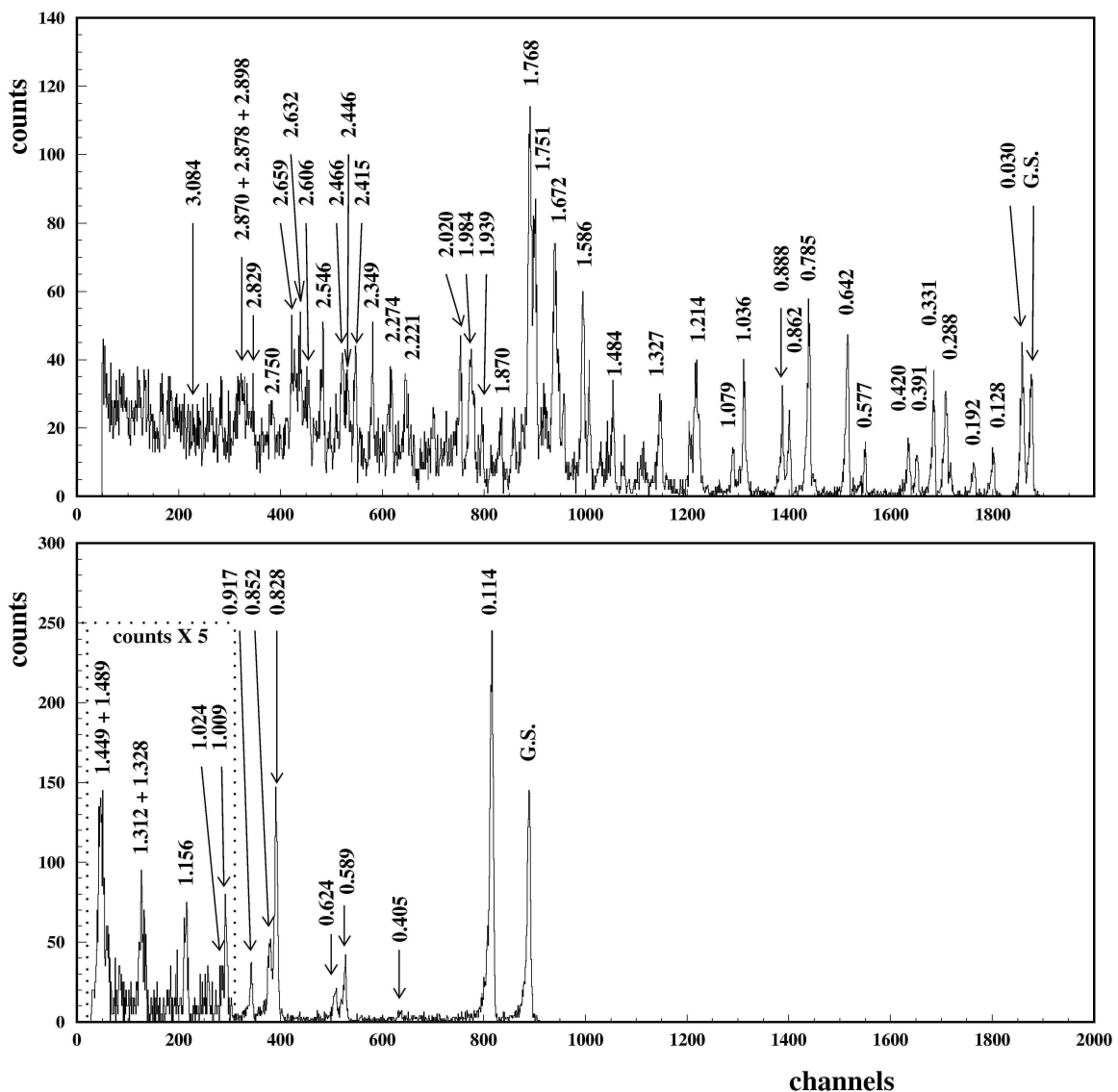


**Figure 1.** Energy spectra of  $\alpha$  particles measured at  $20^\circ$  for the  $^{143}\text{Nd}(p,\alpha)^{140}\text{Pr}$  (top) and  $^{142}\text{Nd}(p,\alpha)^{139}\text{Pr}$  (bottom).

The  $\alpha$  particle position spectra of the  $^{142,143}\text{Nd}(\text{p},\alpha)^{139,140}\text{Pr}$  reactions measured at  $20^\circ$  are shown in Fig.1. The excitation energy of the most prominent peaks is indicated. Transitions to final states of  $^{139}\text{Pr}$  up to an excitation energy of 2.102 MeV and  $^{140}\text{Pr}$  up to 3.118 MeV have been studied. The favorable peak to background ratio, the high resolving power of the magnetic spectrograph, the large solid angle, and the spectrum energy resolution allowed us to measure rather weakly populated levels.

A DWBA analysis of  $\sigma(\theta)$  and  $A_y(\theta)$  has been carried out, assuming a semi-microscopic triton cluster pickup mechanism and using a Gaussian proton-triton interaction potential. Woods-Saxon potentials in entrance and exit channels were used in finite range approximation with the code TWOFNR [10]. In Table 1 the set of the optical model parameters used is listed.

**Table 1.** Woods-Saxon optical model parameters for the incident proton, the outgoing  $\alpha$ -particle, and the geometrical parameters for the bound-state (B.S.) of the transferred triton cluster.

	$V_r$ MeV	$r_r$ fm	$a_r$ fm	$W_v$ MeV	$r_v$ fm	$a_v$ fm	$W_d$ MeV	$r_d$ fm	$a_d$ fm	$V_{so}$ MeV	$r_{so}$ fm	$a_{so}$ fm	$r_c$ fm
p	49.45	1.25	0.696	3.29	1.24	0.51	5.0	1.24	0.51	7.5	1.27	0.467	1.25
$\alpha$	170.0	1.44	0.6	30.0	1.44	0.6							1.30
B.S.		1.40	0.40										

In Fig. 2 experimental and calculated  $\sigma(\theta)$  and  $A_y(\theta)$  for some of the  $^{139}\text{Pr}$  levels have been compared. We have analyzed 37 transitions, of which two doublets and respect to NDS [11] compilation, 7 new levels of  $^{139}\text{Pr}$  have been identified, 11 assignments of  $J^\pi$  have been for the first time performed and 5 ambiguities have been removed.

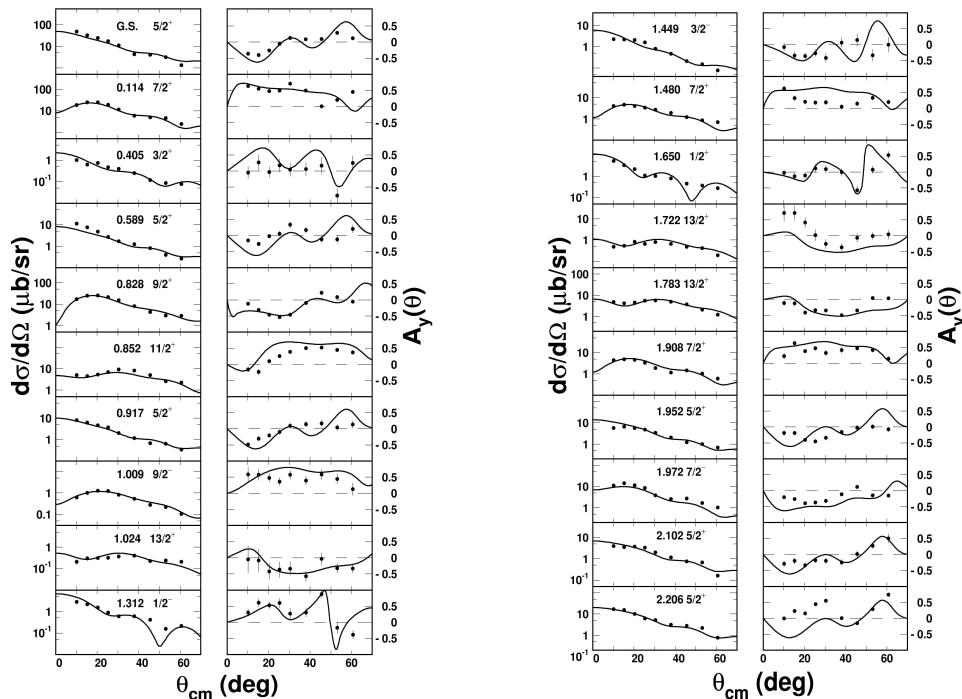


**Figure 2.** Angular distributions of  $\sigma(\theta)$  and  $A_y(\theta)$  for some of the identified levels, whose excitation energy, spin and parity are indicated. The *dots* represent the experimental data, and the *solid lines* the DWBA theoretical estimates.

For this even-even target nucleus only one transferred orbital and total angular momentum  $l$  and  $j$  contribute to the excitation of a given final state. The dependence of  $\sigma(\theta)$  and  $A_y(\theta)$  on the transferred total angular momentum is of the greatest importance for identifying the spin and parity of the levels. The  $J^\pi$  identification of the levels excited in  $(p,\alpha)$  reaction on even-even target nucleus has been performed exploiting the uniqueness of orbital and total angular momentum transfer in the process and the dependence of both  $\sigma(\theta)$  and  $A_y(\theta)$  on the transferred total angular momentum. In particular for  $(p,\alpha)$  reaction, as a general rule, the  $A_y(\theta)$  mean behavior is strictly  $J^\pi$  dependent as shown in Fig. 3 for a hypothetical level at  $E_x=1500$  keV of  $^{139}\text{Pr}$ .

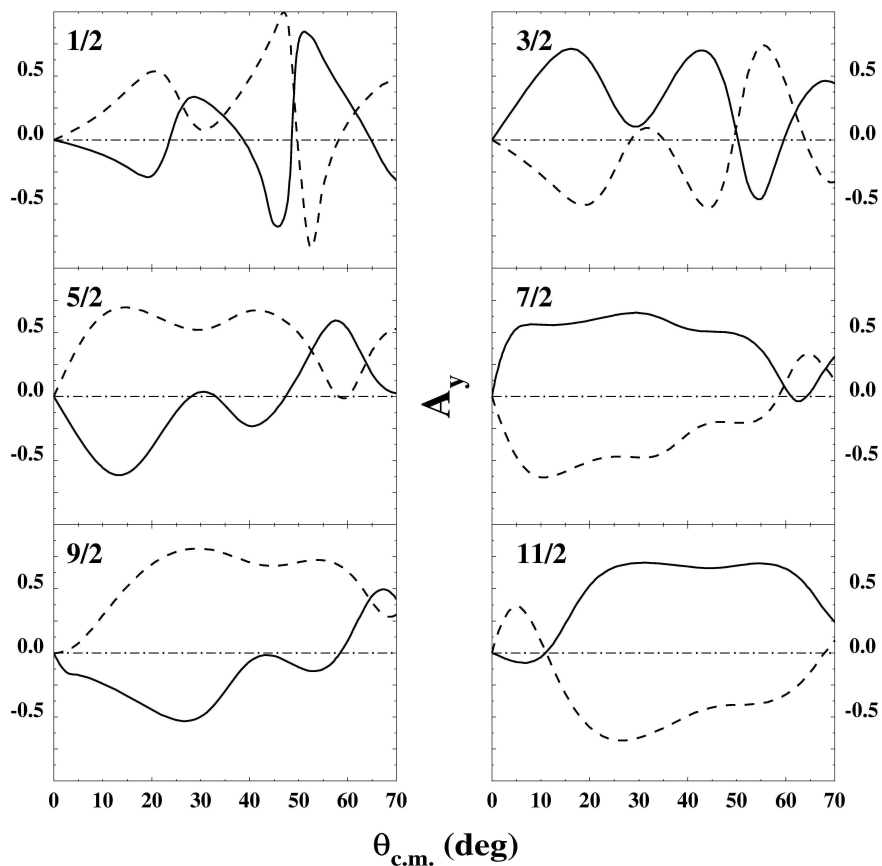


**Figure 3.** Calculated  $A_y(\theta)$  for the  $^{142}\text{Nd}(p,\alpha)^{139}\text{Pr}$  reaction for transitions to a hypothetical level of  $^{139}\text{Pr}$  with given  $J^\pi$  and excitation energy 1500 keV (positive  $\pi$ , solid line; negative  $\pi$ , dotted line).

In the case of an odd-mass target nucleus as  $^{143}\text{Nd}$  and for transitions to states with spin values different from zero, several  $l$  and  $j$  transfers may contribute to each transition, which have to be added incoherently in a DWBA calculation. As a consequence the analysis may be quite complicated and the spectroscopic information less accurate. On the contrary, in the case of homologous states, populated in the  $(p,\alpha)$  reaction on near-magic target nucleus having one nucleon outside a completely filled magic shell as  $^{143}\text{Nd}$ , only one  $l$  and  $j$  transfer is present, the same involved in the transition to the corresponding parent state of  $^{139}\text{Pr}$ .

A remarkable increase of the knowledge of  $^{140}\text{Pr}$  nucleus has been achieved, because 18 new levels have been identified in energy, spin and parity respect to NDS compilation [12]. For the attribution of spin and parity the methodology introduced by our group for homologous states has been applied [5].

Because of the coupling of the  $f_{7/2}$  neutron with the positive parity  $^{139}\text{Pr}$  parent states (G.S.  $5/2^+$ , 0.114 MeV  $7/2^+$ , and 0.828 MeV  $9/2^+$ ) the parity of the  $^{140}\text{Pr}$  homologous states is negative. Multiplets

of states of  $^{140}\text{Pr}$ , homologous to the low-lying states of  $^{139}\text{Pr}$  have been identified. These states, parent and homologous, show significantly different angular distributions of  $\sigma(\theta)$  and  $A_y(\theta)$  to allow a reliable discrimination of the multiplets of homologous states. If the differential cross sections for the transitions belonging to the same multiplet are added, the cumulative cross section is obtained.

In particular we have found:

1) a quintet of states [ $2^-$ ,  $3^-$ ,  $4^-$ ,  $5^-$ ,  $6^-$ ] homologous to the G.S.  $5/2^+$  state of  $^{139}\text{Pr}$ . The  $1^-$  state of the foreseen sextet of homologous states was missing;

2) a sextet of states [ $1^-$ ,  $2^-$ ,  $3^-$ ,  $4^-$ ,  $5^-$ ,  $7^-$ ] homologous to the 0.114 MeV  $7/2^+$  state of  $^{139}\text{Pr}$ . The  $0^-$  and  $6^-$  states of the foreseen octet were missing; the  $\sigma(\theta)$  of the  $6^-$  member of the multiplet is expected to be about 20% of the cumulative cross section of the multiplet, while that of  $0^-$  is expected to be very small and consequently its observation is difficult;

3) a septet of states [ $2^-$ ,  $3^-$ ,  $4^-$ ,  $5^-$ ,  $6^-$ ,  $7^-$ ,  $8^-$ ] homologous to the 0.828 MeV  $9/2^+$  state of  $^{139}\text{Pr}$ . The  $1^-$  state of the foreseen octet was missing, but its integrated cross section is foreseen to be very small.

### 3. The analysis

In the case of weak coupling between parent state and spectator nucleon we expect that:

- $\sigma(\theta)$  and  $A_y(\theta)$  of corresponding homologous states display similar shapes because the process populating these states are basically the same;
- the  $\sigma(\theta)$  of a parent state is equal in magnitude to the cumulative  $\sigma(\theta)$  of the transitions to the multiplet of states homologous to the given parent state;
- the relative cross section for the population of a homologous state with spin  $J_i$  in a given multiplet is proportional to  $(2J_i+1)$ .

In Fig. 4 the comparison between the measured  $\sigma(\theta)$  and  $A_y(\theta)$  for the multiplets of  $^{140}\text{Pr}$  states homologous to the G.S.  $5/2^+$ , 0.114 MeV  $7/2^+$ , and 0.828 MeV  $9/2^+$  parent states of  $^{139}\text{Pr}$  and the measured  $\sigma(\theta)$  and  $A_y(\theta)$  of the  $^{139}\text{Pr}$  parent states is reported. The parent state cross sections are scaled, for each daughter state, by the proper factor  $(2J_i+1)/\sum_i(2J_i+1)$ .

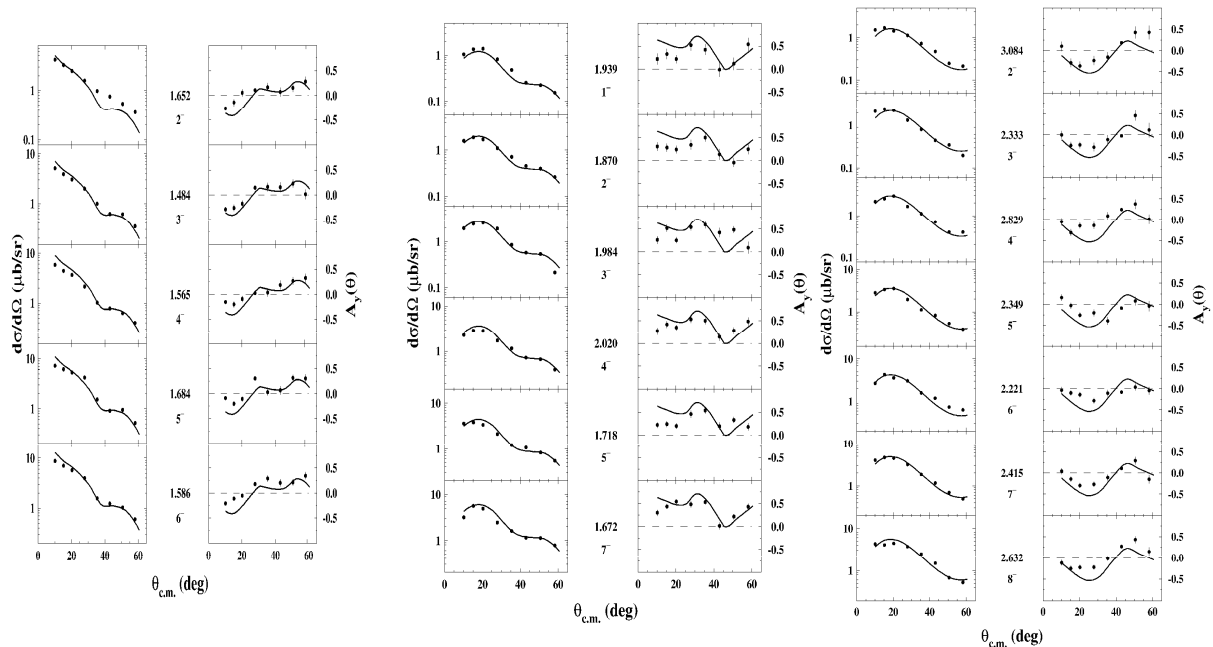


**Figure 4.** Experimental  $\sigma(\theta)$  and  $A_y(\theta)$  (dots) for the population of the quintet of states of  $^{140}\text{Pr}$  homologous to the parent state of  $^{139}\text{Pr}$  G.S.  $5/2^+$ , the sextet of states of  $^{140}\text{Pr}$  homologous to the 0.114 MeV  $7/2^+$  and the septet of states of  $^{140}\text{Pr}$  homologous to the 0.828 MeV  $9/2^+$ , compared with the experimental  $\sigma(\theta)$  and  $A_y(\theta)$  (solid lines) of the corresponding parent states.

In Table 2 knowledge about multiplets of identified homologous states is summarized.

**Table 2.** Multiplets of  $^{140}\text{Pr}$  states homologous to  $^{139}\text{Pr}$  Parent States

A) Parent State: $^{139}\text{Pr}$ G.S. $5/2^+$ ( $\sigma_{\text{int}} = 29.612 \mu\text{b}$ )					
$^{140}\text{Pr}$ Daughter States					
Present work				NDS [12]	
$J\pi$	Exc. energy (MeV)	$\sigma_{\text{int}}$ ( $\mu\text{b}$ )	Branching coeff.	Exc. energy (keV)	$J\pi$
$1^-$	<i>not seen</i>		0.0625		
$2^-$	1.652	3.591	0.1042	1652 <sup>a</sup>	
$3^-$	1.484	4.031	0.1458	1487 . 6	
$4^-$	1.565	4.524	0.1875	1565 <sup>a</sup>	
$5^-$	1.684	6.703	0.2292	1684 <sup>a</sup>	
$6^-$	1.586	7.309	0.2708	1586 <sup>a</sup>	

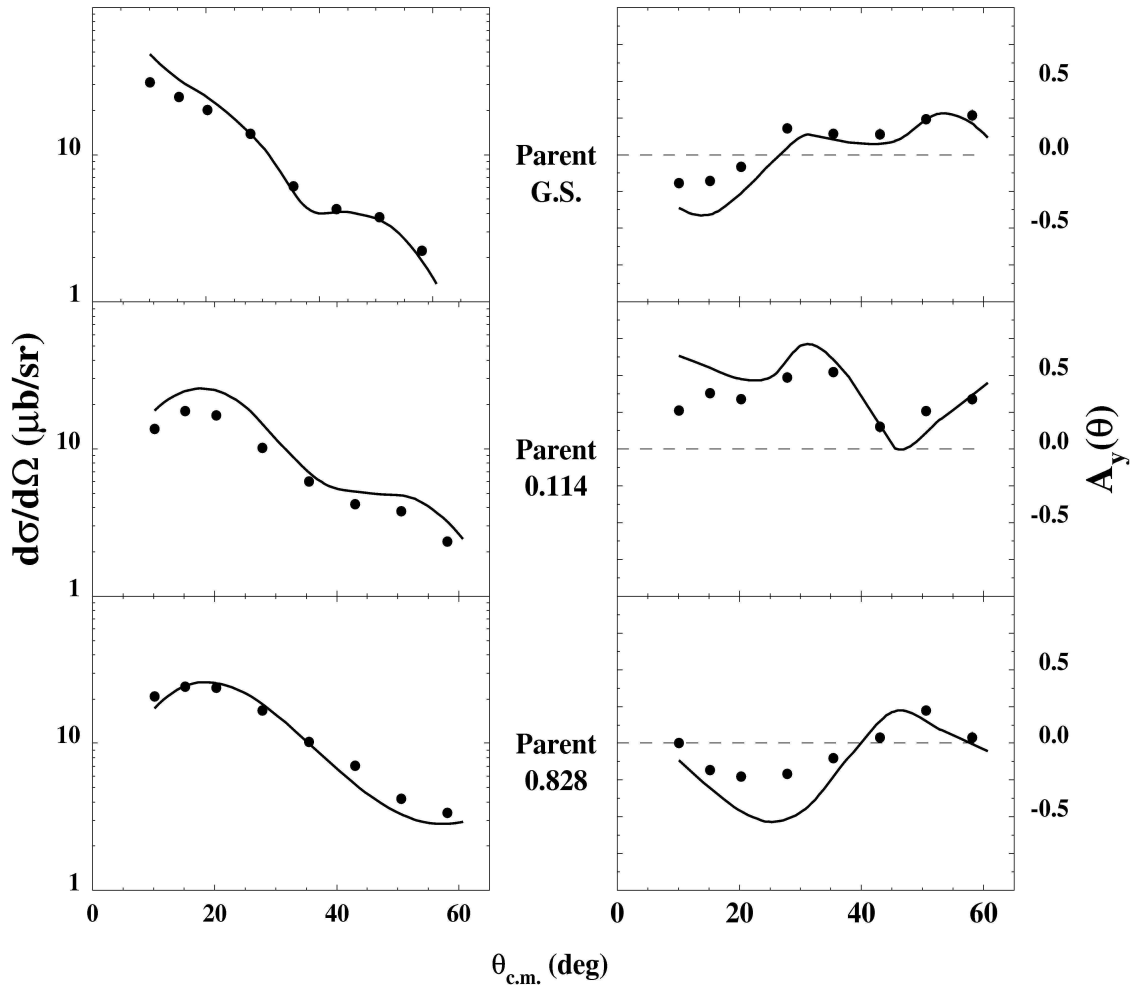
B) Parent State: $^{139}\text{Pr}$ 0.114 MeV $7/2^+$ ( $\sigma_{\text{int}} = 29.333 \mu\text{b}$ )					
$^{140}\text{Pr}$ Daughter States					
Present work				NDS [12]	
$J\pi$	Exc. energy (MeV)	$\sigma_{\text{int}}$ ( $\mu\text{b}$ )	Branching coeff.	Exc. energy (keV)	$J\pi$
$0^-$	<i>not seen</i>		0.0156		
$1^-$	1.939	1.572	0.0469	1939 <sup>a</sup>	
$2^-$	1.870	2.324	0.0781		
$3^-$	1.984	3.168	0.1094	1984 <sup>a</sup>	
$4^-$	2.020	3.677	0.1406	2020 <sup>a</sup>	
$5^-$	1.718	4.602	0.1719	1718 <sup>a</sup>	
$6^-$	<i>not seen</i>		0.2031		
$7^-$	1.672	5.965	0.2344	1672 <sup>a</sup>	

C) Parent State: $^{139}\text{Pr}$ 0.828 MeV $9/2^+$ ( $\sigma_{\text{int}} = 31.450 \mu\text{b}$ )					
$^{140}\text{Pr}$ Daughter States					
Present work				NDS [12]	
$J\pi$	Exc. energy (MeV)	$\sigma_{\text{int}}$ ( $\mu\text{b}$ )	Branching coeff.	Exc. energy (keV)	$J\pi$
$1^-$	<i>not seen</i>		0.0375		
$2^-$	3.084	2.120	0.0625		
$3^-$	2.333	2.654	0.0875	2333 <sup>a</sup>	
$4^-$	2.829	3.400	0.1125	2822 <sup>a</sup>	
$5^-$	2.349	3.973	0.1375	2349 <sup>a</sup>	
$6^-$	2.221	5.296	0.1625	2221 <sup>a</sup>	
$7^-$	2.415	5.725	0.1875	2416 <sup>a</sup>	
$8^-$	2.632	8.548	0.2125	2632 <sup>a</sup>	

<sup>a</sup> This energy value, reported in NDS [12], belongs to our preliminary measurement at  $\theta_{\text{lab}} = 20^\circ$ .

In Fig. 5 the cumulative cross sections and analyzing powers for the three identified multiplets of homologous states are compared with the cross sections and analyzing powers of the corresponding parent state. Good agreement is achieved both in shape and in absolute values, except for the cumulative cross section of the sextet of states  $[1^-, 2^-, 3^-, 4^-, 5^-, 7^-]$  homologous to the 0.114 MeV  $7/2^+$  state of  $^{139}\text{Pr}$ . In this case the cumulative cross section of the multiplet of states homologous to the  $^{139}\text{Pr}$  parent state does not exhaust the parent state cross section, due to the absence of  $6^-$  daughter state.



**Figure 5** Cumulative cross sections and analyzing powers for population of multiplets of states of  $^{140}\text{Pr}$  (dots) homologous to the low-lying parent states of  $^{139}\text{Pr}$ , compared with experimental cross sections and analyzing powers for population of these  $^{139}\text{Pr}$  states (solid lines).

The weak coupling model foresees that the cross section of a homologous state with spin  $J_i$  in a given multiplet is related to that of the corresponding parent state by the following relation:

$$\sigma_{\text{daughter}}(^{140}\text{Pr}, J_i) = \sigma_{\text{parent}}(^{139}\text{Pr}) \times (2J_i+1) / \sum_i(2J_i+1)$$

In Fig. 6 the quantities  $[\sigma(J_i)_{^{140}\text{Pr}} / \sigma_{^{139}\text{Pr}}] \times \sum_i(2J_i+1)$  are reported for each multiplet vs.  $J_i$ , together with the straight  $(2J_i+1)$  line. The predicted proportionality of the reduced experimental values  $[\sigma_{\text{daughter}} / \sigma_{\text{parent}}] \times \sum_i(2J_i+1)$  for the identified multiplets with the  $(2J_i+1)$ , strongly supports the present spin and parity assignments of the 18 states of  $^{140}\text{Pr}$ , for the first time identified in  $J^\pi$ .

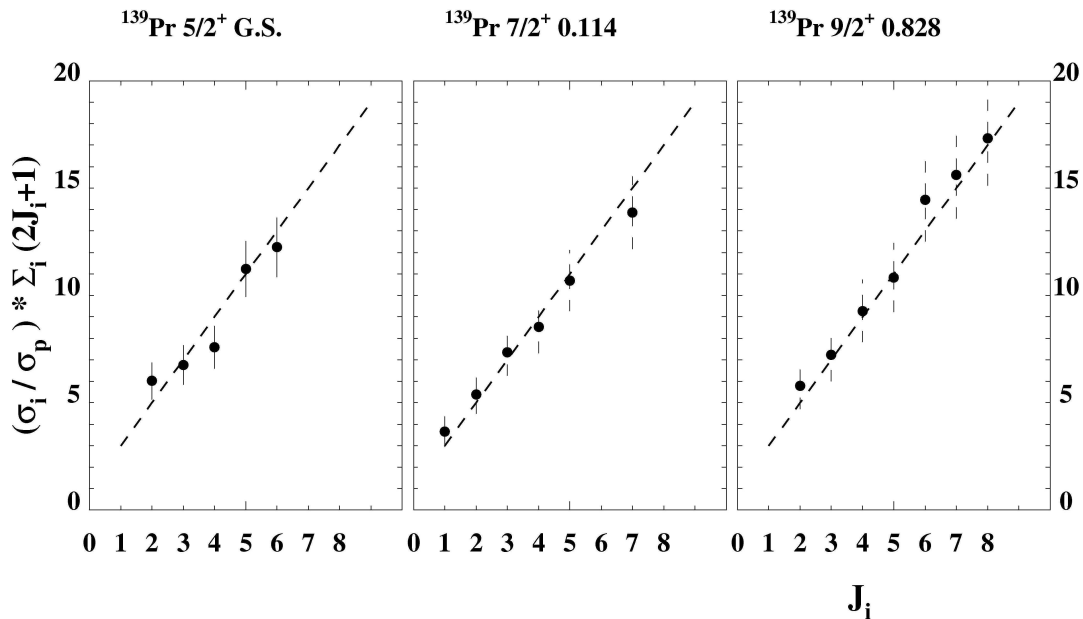


**Figure 6.** Experimental values  $[\sigma(J_i)_{140\text{Pr}}/\sigma_{139\text{Pr}}] \times \sum_i(2J_i+1)$  (dots) for the multiplets of states homologous to the  $^{139}\text{Pr}$  parent states reported as a function of  $J_i$  and compared with the  $(2J_i+1)$  straight line predicted by the weak coupling model (*dotted lines*).

#### 4. References

- [1] Guazzoni P, Zetta L, Demetriou P and Hodgson P E 1996 *Z. Phys. A* **354** 53
- [2] Guazzoni P, Zetta L, Della Vedova F, Lenzi S M, Vitturi A, Graw G, Hertenberger R, Wirth H-F and Jaskola M 2005 *Proc. 16th Inter. Spin Physics Symposium – Spin 2004* (Singapore: World Scientific) p 665
- [3] Guazzoni P, Jaskola M, Zetta L, Gu J N, Vitturi A, Graw G, Hertenberger R, Schiemenz P, Valnion B, Atzrott U and Staudt G 1998 *Eur. Phys. J. A* **1** 365
- [4] Guazzoni P, Jaskola M, Zetta L, Gu J N, Vitturi A, Graw G, Hertenberger R, Hofer D, Schiemenz P, Valnion B, Atzrott U, Staudt G and Cata Danil G 1997 *Z. Phys. A* **350** 381
- [5] Guazzoni P, Zetta L, Bayman B F, Covello A, Gargano A, Graw G, Hertenberger R, Wirth H-F and Jaskola M 2005 *Phys. Rev. C* **72** 044604
- [6] Gu J N, Vitturi A, Zhang C H, Guazzoni P, Zetta L, Graw G, Jaskola M and Staudt G 1997 *Phys. Rev. C* **55** 2395
- [7] von Ehrenstein D 1970 *Phys. Rev. C* **1** 2066
- [8] Hertenberger R, Metz A, Eisermann Y, El Abiary K, Ludewig A, Pertl C, Trieb S, Wirth H-F, Schiemenz P and Graw G 2005 *Nucl. Instrum. Methods Phys. Res. A* **536** 266
- [9] Wirth H F, Angerer H, von Egidy T, Eisermann Y, Graw G and Hertenberger R 2001, *Jahresberichth 2000*, Beschleunigerlaboratorium München p 71
- [10] Igarashi M 1977 *Computer code TWOFNR* unpublished.
- [11] Burrows T W 2001 *Nuclear Data Sheets* **92** 623
- [12] Nica N 2007 *Nuclear Data Sheets* **108** 1287